

# MICRO-MECHANICAL PERFORMANCE OF CONCRETE USED AS RECYCLED RAW MATERIAL IN CEMENTITIOUS COMPOSITE

VLADIMÍR HRBEK<sup>a,b,\*</sup>, VERONIKA KOUDELKOVÁ<sup>a,b</sup>, ZDENĚK PROŠEK<sup>a,c</sup>,  
PAVEL TESÁREK<sup>a</sup>

<sup>a</sup> Czech Technical University in Prague, Faculty of Civil Engineering, Thákurova 7, 166 29 Prague 6, Czech Republic

<sup>b</sup> Institute of Theoretical and Applied Mechanics AS CR, v.v.i., Prosecká 76, 190 00 Prague 9, Czech Republic

<sup>c</sup> University Centre for Energy Efficient Buildings of Czech Technical University in Prague, Třinecká 1024, 273 43 Buštěhrad, Czech Republic

\* corresponding author: [vladimir.hrbek@fsv.cvut.cz](mailto:vladimir.hrbek@fsv.cvut.cz)

**ABSTRACT.** The reduction of industrial pollution is recently one of main goals over all fields. In civil engineering, re-cycling of structural waste provides wide opportunity contributing this effort. This paper focus on re-use of concrete waste, which after further processing can be used in new constructions as partial supplement to the mixture. To investigate the impact of re-cycled concrete addition, it is necessary to determine mechanical and structural parameters of individual phases in the “raw” material. For this purpose, grid indentation and scanning electron microscopy with energy-dispersive X-ray spectroscopy (SEM, EDX) are combined to determine properties of concrete sample.

**KEYWORDS:** re-cycled concrete, grid indentation, SEM, EDX, image analysis.

## 1. INTRODUCTION

The waste material accumulation became worldwide environmental and economical problem. Development of new effective and thrifty methods for re-use of waste products lowers the number of waste deposits while saving natural sources and environment. For example, in 2012, the countries of European Union produced over 2.5 billion tones of waste and managed to recycle barely 10% of this amount. In case of Czech Republic, over 23 million tones of waste were produced and slightly over one-fifth recycled (statistics according to Environmental Data Center on Waste).

One of main problems with incorporation of waste materials in civil engineering (especially in constructions) is mistrust of designers and developers toward recycled construction waste. Despite lower price of these materials (compare to traditional raw materials), final cost can be paradoxically higher due to the transportation [1–3].

The solid phase of concrete is made of coarse and fine aggregate (65 to 70%) and cement paste. Typically, when recycled, coarse aggregate (30 to 50% of raw material) is to be reused, which leaves majority of the concrete as secondary waste product [4]. Complete recycling of concrete (concretely use of high-speed milling) can turn this waste into fine powder (fraction < 1 mm) with potential usage as micro-filler (fine ground hydration products and fine aggregate) and partial cement substitute (non-hydrated clinker in cement paste). Nevertheless, the processing itself is complicated and bears addition financial costs. Beyond that, due to the lack of studies and short

experience of civil engineering practice with such fine powdered material, the implementation of recycled secondary waste material is not possible on large scale.

M. Chen et al. [5] used the recycled concrete fine powder in their study as full substitute of pulverized limestone in asphalt mixture. The results of X-ray diffraction and scanning electron microscopy (SEM) showed higher content of SiO<sub>2</sub>, lower CaCO<sub>3</sub> content and rougher partical surface in recycled concrete fine powder, compare to of pulverized limestone. When used as filler in asphalt mixture, the water sensitivity of samples reduced while mechanical properties in high temperatures and fatigue persistence increased. However, mechanical properties in low temperature slightly decreased.

In case of cement based mixtures, recycled concrete fine powder serves much as a micro-filler, which acts as coarse aggregate on the mezo- and micro-scale of the material. Unfortunately, studies about recycled micro-fillers are not yet carried out, although the idea seems promising as replacement of current micro-filling agents [6]. Moreover, the potential of non-hydrated clinker present in the powder was so far vastly ignored.

Y. J. Kim et al. [7] presented in his study features of cement paste modified by recycled concrete fine powder as a partial replacement for a binder. According to the results, workability in mixture’s fresh state decreased with increasing level of cement compensation and the hydration process was delayed up to 2 hours. In case where 45% of cement was replaced by recycled concrete fine powder, the mechanical com-

pressive strength reduced to 30% while absorptivity gain reached almost 70%. The conclusion of this study proposed limitation of the replacement to 15%.

M. Lidmila a K. Šeps [8–10] used in their studies pulverized concrete recycled from railway sleepers. The product of recycling showed low reactive potential very likely due to very fine milling of the concrete, i.e. unfolding of non-hydrated clinkers. As the level of non-hydrated clinker is low, the material is to be possibly used for strengthening of subsoil under railway structures [11]. Other potential utilization, in small-scale, can be found in cementitious composite material.

The knowledge of the material on the micro-scale is thus crucial to understand the composite's behavior on higher scale levels. With such level of investigation, it is possible to develop up-scaled prediction of macro-mechanical properties, as well as optimize the efficiency of used fine powdered concrete recycle product. This study is focused on investigation of micro-mechanical and micro-structural performance of the in-put "raw" material, i.e. concrete sleepers intended for recycle. The output would serve as comparative analysis to further planned research of the recycled pulverized concrete.

## 2. MATERIAL

On of raw materials used for the recycled pulverized concrete are railway sleepers type PB2 and SB8 (used in this study, Fig. 1a). It the first step of the recycling process, crude recycled concrete gravel with dimension 0–32 mm (Fig. 1b) arises from the kibble of the sleepers and the metallic parts and reinforcement is separated. After selection of finer concrete gravel (fraction 0–16 mm, Fig. 1c), the material is milled in two steps to the final product (recycled pulverized concrete, fraction 0–1 mm). The fine milling of the material was delivered by company Lavaris Ltd. (procedure protected by patents act) using the high speed milling technique.

For a purpose of the investigation, piece of crude concrete gravel (Fig. 1b) was embedded in epoxy resin and let to harden for approx. 24 hours. A part of the specimen was than severed (approx. thickness 15 mm) and silica-carbon papers and diamond suspensions were used for grinding and polishing of the specimen surface. This technique ensured adequate surface roughness of the sample for both indentation and SEM investigation. The coordination mark was inscribe on the polished surface, serving as origin for further orientation. This enabled positioning of both investigation techniques in the very like area of the sample.

## 3. INVESTIGATION PROCEDURE

The investigation of the crude recycled concrete consisted of three main techniques, instrumental indentation, scanning electron microscopy combined with



(A) . Railway sleepers, type PB8.



(B) . Crude recycled concrete (0 - 32 mm)

(C) . "Raw" recycled concrete (0 - 16 mm)

FIGURE 1. Products of concrete recycling procedure.

electron probe microanalysis (SEM EPMA) and back scattered electron micrographs (SEM BSE) image processing. As a result, combination of micromechanical properties, phases chemical composition and material structure enabled proper description of the material.

### 3.1. SCANNING ELECTRON MICROSCOPY

The scanning electron microscopy (SEM) investigation was performed in MIRA II LMU (Tescan corp., Brno) on polished specimens coated with thin layer of carbon necessary to ensure proper conductivity of the surface. Working distance of the microscope was set closely to 15 mm and accelerating voltage was set to 15 kV – to provide good signal.

Chemical composition (in weight percentage) of each phase characterized by the same level of grey scale was determined using EPMA based on the detection of the X-rays by energy dispersive X-ray detector (EDX, Bruker corp., Berlin) on several point of each position.

Due to the time-demands of technique such as phase determination by EPMA, image analysis of SEM BSE micrographs was used to obtain phase volumetric representations in viewed field, i.e. material structure. The micrographs were acquired at different magnifications. The approximate area of indentation was investigated at first at the magnification 600× to gain adequate overview. Than the area was scanned with higher magnification (above 1200×) for detailed study of indented positions in several images. The SEM micrographs acquired with back scattered electron detector (BSE) provide information about distribution (and chemical composition) of different phases due to different spectrum of the back scattering coefficient.

### 3.2. QUASI-STATIC NANO-INDENTATION

The technique of nano-indentation (Ti 7500 series, Hysitron Inc.) was selected for evaluation of microscale elastic properties of the material. Its principal is based on dependency of probe propagation with respect to the recorded force. The force-displacement record is further further processed and the mechanical properties are calculated from the unloading part of the record. Incorporated errors of the measurement, such as creep and visco-elasticity of measured phases, is avoided by appropriate test setup [12–18]. For purpose of this study, the load function kept for further described indentation similar, i.e. the “loading” and “unloading” segments lasted 5 seconds each with an in-between 60 seconds “holding” time segment. The measurement was performed in two major steps (Level I and II) to achieve efficient investigation of phases on different material levels.

As an early step, a load-controlled quasi-static grid indentation was performed with an applied force of 10 mN (almost maximum capacity of the transducer) to obtain route-identification of the material. The indents were each separated by 25  $\mu\text{m}$  in 10 by 10 raster, which allowed both micro-mechanical evaluation of phases in large range and estimation of further used indentation depth. However, such setting does not meet the grid-indentation specifications of heterogeneous composite [19–22], particularly does not guarantee consistent half-space influenced by each indent.

The first step (Level I) was thus selected as displacement-driven quasi-static grid measurement with each indent driven into 150 nm depth in two positions. The grid was constructed of 21 by 21 indents pattern with 5  $\mu\text{m}$  spacing. The setting ensured equal indented half-space volume of material represented on the sample surface by circle with  $6 \times$  indentation depth diameter [19]. The indentation covered space over the total investigated area (given by the grid dimensions 100 by 100  $\mu\text{m}$ ) was computed equal to 2.81% (ratio of efficiency).

The second step (also displacement-driven with identical indentation depth - Level II) was therefore designed for detailed investigation of selected position. The grid consisted of 25 by 25 indents separated by 2  $\mu\text{m}$  and the efficiency equaled to 17.26%. The setting (especially location and size of the position) aimed for close evaluation of phases present in cement paste.

## 4. RESULTS INTERPRETATION

The SEM EPMA EDX analysis of 41 material positions showed five main phases present in the investigated material, i.e. low-density and high-density calcium-silica-hydrate (LD C-S-H and HD C-S-H), calcium hydroxide (CH), non-hydrated clinker and aggregate – potassium and sodium feldspar and quartz (Fig. 2). The phases average weight percentage of each element are summarized in Tab. 1.

Moreover, 1.25 mm by 1.25 mm area, where level I indentation positions are expected, was sequentially

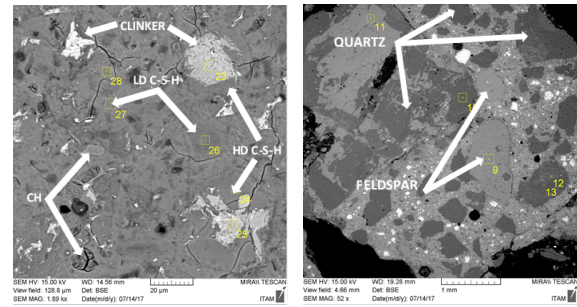
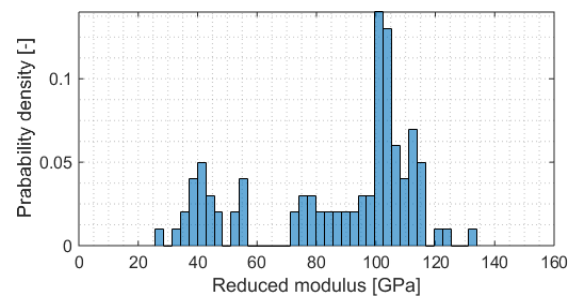


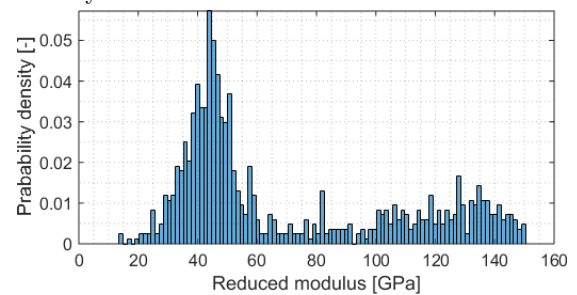
FIGURE 2. Micrographs with identified material phases.

scanned in BSE mode with high resolution ( $5 \times 5$  sequence of 250  $\mu\text{m}$  wide images). The reconstruction of this area enabled exact linkage between indentation data material structure.

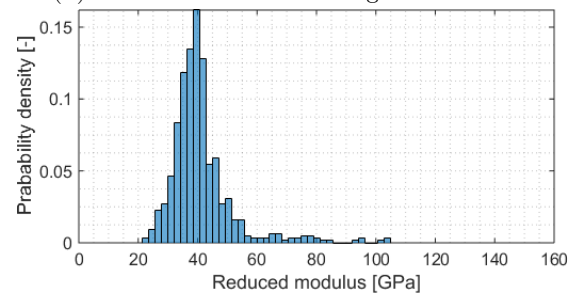
The histograms of nano-indentation results, the indentation modulus in particular, were normalized in respect to the 0.1 of minimum value, as captured for all studied levels in Fig. 3. The preliminary study of the material (Fig. 3a) proved to insufficiently detail mechanical properties of all phases.



(A) . Reduced modulus histogram – Preliminary study.



(B) . Reduced modulus histogram – Level I.



(C) . Reduced modulus histogram – Level II.

FIGURE 3. Histograms of indentation modulus

This can be observed in comparison with level I

Element	Quartz	Potassium Feldspar	Sodium Feldspar	LD C-S-H	HD C-S-H	CH	Clinker
Ca			6.65	37.37	45.37	60.05	50.18
Si	46.74	29.39	27.24	6.41	12.83	0.35	12.42
Al		10.09	11.06	1.42	1.33		0.50
Mg				0.35	0.71	0.32	0.40
Na		0.87	8.09	0.11	0.24		
K		14.01	0.52	0.33	0.35		0.52
S				2.24	0.81	0.16	
Cl					0.36		
Fe				1.21	1.05	1.13	0.48
O	53.26	45.63	46.45	50.56	36.95	37.99	35.50

TABLE 1. Average weight percentage of elements present in phases.

of the study (Fig. 3b). The results, in this case, are more likely to depict the material structure as the occurrence of reduced modulus around 40 GPa is most frequent (see [23–26]). Also, several peaks corresponding to number of phases identified by SEM analysis can be found in the histogram.

The Level II of the material was focused mostly on the investigation of cement paste, especially on CSH and CH phase. Again, Fig. 3c confirms predominant representation of high-density calcium-silica-hydrate in the matrix.

The overall results (Fig. 4), as combination of both measured levels, gives detailed view of micromechanical performance of the material. The probability density function of measured indentation moduli was subsequently processed with spectral deconvolution in order to obtain Gaussian distribution of expected phases. The mechanical properties of Phases 1-5 in Fig. 4 were thus determined as:

Phase 1 =  $19.17 \pm 3.54$  GPa = LD C-S-H

Phase 2 =  $39.75 \pm 5.98$  GPa = HD C-S-H

Phase 3 =  $58.59 \pm 6.34$  GPa = calcium hydroxide

Phase 4 =  $79.78 \pm 3.11$  GPa = presumably aggregate

Phase 5 =  $118.35 \pm 16.85$  GPa = clinker

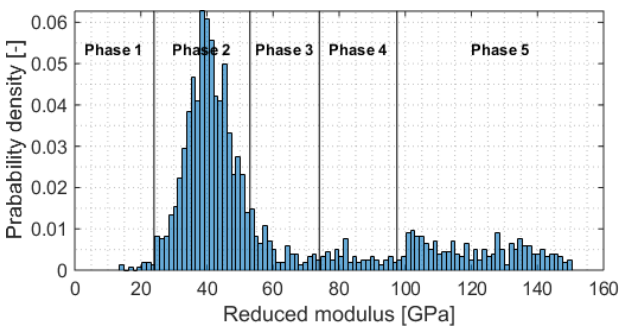


FIGURE 4. Histogram of overall reduced modulus results.

The results are consistent with previously published researches [23–32]. Based on these results, maps of indentation moduli over the investigated positions (Fig. 5–6) were constructed with bordering conditions

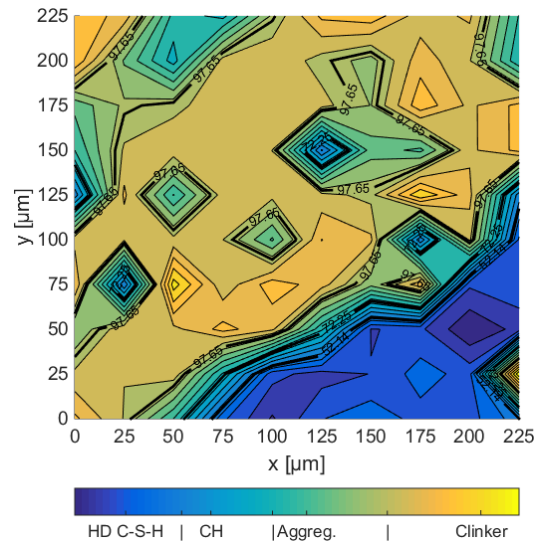


FIGURE 5. Contour map of preliminary results.

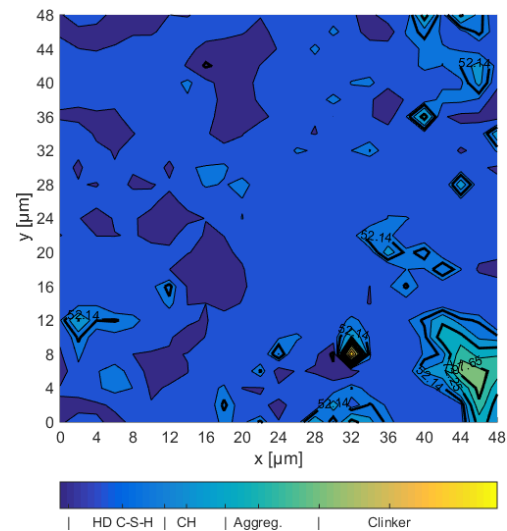


FIGURE 6. Contour map of results on level II.

identical to limits in Fig. 4. In addition, it was possible to link maps of indentation data to particular segments of SEM BSE micrographs (Fig. 7).

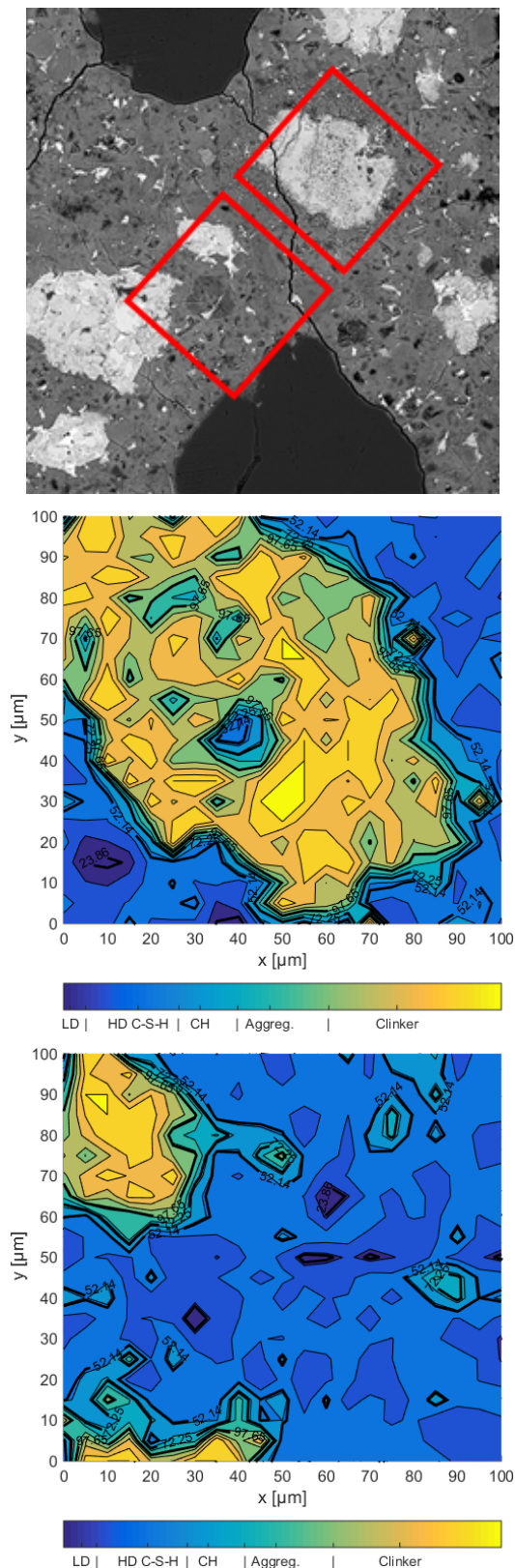


FIGURE 7. Contour maps of level I results linked to the SEM BSE micrograph.

## 5. CONCLUSION

The raw material (railway sleeper PB8) used after milling as recycled pulverized concrete in cementitious composites was in focus of this study. The

micromechanical properties and material structure of this base material were investigated with combined methodology to predict performance when used as filler and cement replacement.

The scanning electron microscopy methods (SEM EPMA EDX, BSE) were used to determine chemical and structural composition of the material (unknown prior to the investigation). Therefore, low- and high-density calcium-silica-hydrate (LD / HD C-S-H), calcium hydroxide (CH), three aggregate types and non-hydrated clinker were identified as main material phases.

The nanoindentation technique over two main material levels enabled evaluation of the indentation modulus of these phases due to the spectral deconvolution of measured data. Reverse reconstruction of indented areas with respect to deconvolution results let to interlink of indentation and BSE diagrams. Although the combined investigation provided sufficient results, more detail should be obtained in case of aggregate phases prior to modeling of the material.

## LIST OF SYMBOLS

$F$	Applied force [ $\mu\text{N}$ ]
$h_i$	Indentation depth [nm]
$E_r$	Reduced modulus [GPa]
$H$	Hardness [GPa]
$h_c$	Contact depth [nm]

## ACKNOWLEDGEMENTS

The research is financially supported by Czech Technical University in Prague – project SGS17/168/OHK1/3T/11 and by the Czech Science Foundation research project 17-06771S. The support is gratefully appreciated.

## REFERENCES

- [1] M. Stibůrek. Možnosti využití stavebních odpadů. *Beton TKS* **2**:45–47, 2008.
- [2] S. Marinković, et al. Comparative environmental assessment of natural and recycled aggregate concrete. *Waste Management* **30**(11):2255–2264, 2010. DOI:<https://doi.org/10.1016/j.wasman.2010.04.012>.
- [3] N. Tošić, et al. Multicriteria optimization of natural and recycled aggregate concrete for structural use. *Journal of Cleaner Production* **87**(1):1–11, 2014. DOI:<https://doi.org/10.1016/j.jclepro.2014.10.070>.
- [4] C. S. Poon, et al. Effect of microstructure of itz on compressive strength of concrete prepared with recycled aggregates. *Construction and Building Materials* **18**(6):461–468, 2004. DOI:<https://doi.org/10.1016/j.conbuildmat.2004.03.005>.
- [5] M. Chen, et al. Potential of recycled fine aggregates powder as filler in asphalt mixture. *Construction and Building Materials* **25**(10):3909–3914, 2011. DOI:<https://doi.org/10.1016/j.conbuildmat.2011.04.022>.
- [6] J. Topič, Z. Prošek. Properties and microstructure of cement paste including recycled concrete powder. *Acta Polytechnica* **57**(1):49–57, 2017. DOI:<https://doi.org/10.14311/AP.2017.57.0049>.

- [7] Y. J. Kim, et al. Utilization of waste concrete powder as a substitution material for cement. *Construction and Building Materials* **30**:500–504, 2012.  
DOI:https://doi.org/10.1016/j.conbuildmat.2011.11.042.
- [8] M. Lidmila, et al. Utilization of recycled fine-ground concrete from railway sleepers for production of cement-based binder. *Applied Mechanics and Materials* **486**:323–326, 2014.  
DOI:doi.org/10.4028/www.scientific.net/AMM.486.323.
- [9] K. Šeps, et al. Mechanical properties of mixtures with crushed sleepers stiffened by synthetic fibers. In *4th Conference on Nano and Macro Mechanics*, pp. 193–198. 2013.
- [10] M. Lidmila, K. Šeps. Použití směsí s recyklovaným betonem jako stabilizované vrstvy. In *Conference Nanomateriály a nanotechnologie ve stavebnictví 2013*, pp. 103–107. 2013.
- [11] M. Lidmila, et al. Utilization of recycled binder for improvement of subsoil under railway sleepers. *Applied Mechanics and Materials* **825**:53–56, 2016.  
DOI:doi.org/10.4028/www.scientific.net/AMM.825.53.
- [12] J. W. Harding, I. N. Sneddon. The elastic stresses produced by the indentation of the plane surface of a semi-infinite elastic solid by a rigid punch. *Mathematical Proceedings of the Cambridge Philosophical Society* **41**(1):16–26, 1945.  
DOI:https://doi.org/10.1017/S0305004100022325.
- [13] W. Oliver, G. M. Pharr. An improved technique for determining hardness and elastic modulus using load and displacement sensing indentation measurements. *Journal of Material Research* **7**(6):1564–1583, 1992.  
DOI:https://doi.org/10.1557/JMR.1992.1564.
- [14] J. Woigard, J. C. Dargenton. An alternative method for penetration depth determination in nanoindentation measurement. *Journal of Material Research* **12**(9):2455–2458, 1997.  
DOI:https://doi.org/10.1557/JMR.1997.0324.
- [15] J. L. Hay, G. Pharr. *ASM Handbook Volume 8: Mechanical Testing and Evaluation*. 10th edition. ASM International, Materials Park, OH, 2000.
- [16] G. M. Pharr, A. Bolshakov. Understanding nanoindentation unloading curves. *Journal of Material Research* **17**(10):2660–2671, 2002.  
DOI:https://doi.org/10.1557/JMR.2002.0386.
- [17] W. Oliver, G. M. Pharr. Measuring of hardness and elastic modulus by instrumented indentation: Advances in understanding and refinement of methodology. *Journal of Material Research* **19**(1):3–20, 2004.  
DOI:https://doi.org/10.1557/jmr.2004.19.1.3.
- [18] A. C. Fischer-Cripps. A simple phenomenological approach to nanoindentation creep. *Journal of Material Science and Engineering A* **385**(1-2):74–82, 2004.  
DOI:https://doi.org/10.1016/j.msea.2004.04.070.
- [19] G. Constantinides, K. R. Chandran, F.-J. Ulm, K. okJ. Van Vliet. Grid indentation analysis of composite microstructure and mechanics: Principles and validation. *Journal of Material Science and Engineering A* **430**(1-2):189–202, 2006.  
DOI:https://doi.org/10.1016/j.msea.2006.05.125.
- [20] F.-J. Ulm, M. Vandamme, C. Bobko, et al. Statistical indentation techniques for hydrated nanocomposites: Concrete, bone and shale. *Journal of the American Ceramic Society* **90**(9):2677–2692, 2007.  
DOI:https://doi.org/10.1111/j.1551-2916.2007.02012.x.
- [21] J. Nohava, P. Haušild, Š. Houdková, R. Enžl. Comparison of isolated indentation and grid indentation methods for hvof sprayed cermets. *Journal of Thermal Spray Technology* **21**(3-4):651–658, 2012.  
DOI:10.1007/s11666-012-9733-6.
- [22] L. S. de Vasconcelos, R. Xu, J. Li, K. Zhao. Grid indentation analysis of mechanical properties of composite electrodes in li-ion batteries. *Extreme Mechanics Letters* **9**(3):495–502, 2016.  
DOI:https://doi.org/10.1016/j.eml.2016.03.002.
- [23] O. Bernard, F.-J. Ulm, E. Lemarchand. A multiscale micromechanics-hydration model for the early-age elastic properties of cement-based materials. *Cement and Concrete Research* **33**(9):1293–1309, 2003.  
DOI:https://doi.org/10.1016/S0008-8846(03)00039-5.
- [24] W. Zhu, J. J. Hughes, N. Bicanic, C. J. Pearce. Nanoindentation mapping of mechanical properties of cement paste and natural rocks. *Materials Characterization* **58**(11-12):1189–1198, 2007.  
DOI:https://doi.org/10.1016/j.matchar.2007.05.018.
- [25] L. Sorelli, G. Constantinides, F.-J. Ulm, F. Toutlemonde. The nano-mechanical signature of ultra high performance concrete by statistical nanoindentation techniques. *Cement and Concrete Research* **38**(12):1447–1456, 2008.  
DOI:https://doi.org/10.1016/j.cemconres.2008.09.002.
- [26] D. Davydov, M. Jirásek, L. Kopecký. Critical aspects of nano-indentation technique in application to hardened cement paste. *Cement and Concrete Research* **4**(1):20–29, 2011.  
DOI:https://doi.org/10.1016/j.cemconres.2010.09.001.
- [27] P. Tesárek, J. Němeček. Microstructural and micromechanical study of gypsum. *Chem Listy* **105**:552–553, 2011.
- [28] P. Tesárek, et al. Micromechanical properties of different materials on gypsum basis. *Chem Listy* **106**:547–548, 2012.
- [29] N. P. Daphalapurkar, F. Wang, B. Fu, et al. Determination of mechanical properties of sand grains by nanoindentation. *Experimental Mechanics* **51**(5):719–728, 2011.  
DOI:https://doi.org/10.1007/s11340-010-9373-z.
- [30] W. Pabst, E. Gregorová. Elastic properties of silica polymorphs - a review. *Ceramics - Silicates* **57**(3):167–184, 2013.
- [31] P. Acker. Micromechanical analysis of creep and shrinkage mechanisms. In *6th International Conference on Creep, Shrinkage and Durability Mechanics of Concrete and Other Quasi-Brittle Materials*, pp. 15–25. Cambridge, USA, 2001.
- [32] K. Velez, S. Maximilien, D. Damidot, et al. Determination by nanoindentation of elastic modulus and hardness of pure constituents of portland cement clinker. *Cement and Concrete Research* **31**(4):555–561, 2001.  
DOI:https://doi.org/10.1016/S0008-8846(00)00505-6.